Switching Devices Comparison and RC Snubber for Ringing Suppression in one Single Leg T-type Converter

Yong Liu[1], Fan Fei[2], Kye Yak See[2], Xiong Liu[3], Ziyou Lim[1], Rejeki Simanjorang[3], Josep Pou[2], Amit K. Gupta[3], Jih-Sheng Lai[4]
[1]Rolls-Royce @ NTU Corporate Lab, Nanyang Technological University, Singapore
[2]School of Electrical and Electronic Engineering, Nanyang Technological University, Singapore
[3]Applied Technology Group, Rolls-Royce Singapore Pte. Ltd, Singapore
[4]Future Energy Electronics Center, Virginia Tech, Blacksburg, VA, USA
LIUY0111@e.ntu.edu.sg

***Abstract*—In this paper, one single leg T-type converter with full silicon carbide (SiC) half-bridge power modules and hybrid power modules combined silicon carbide (SiC) with silicon (Si) power module, are designed and investigated. Firstly, the switching characteristics of Cree SiC device CAS300M12BM2 and Semikron SiC device SKM350MB120SCH17 single-leg T-Type converters are compared with double pulse testing (DPT). Then, to further investigate the performance, the hybrid power modules of the single leg T-type converter with Cree SiC device CAS300M12BM2 and Semikron Si device SKM300GM12T4 are built, which can increases the power density, compared to the full SiC devices T-type converter. To suppress the ringing of the middle leg switching device, the resistor-capacitor (RC) snubber are designed and demonstrated with DPT. Finally, the function testing of the hybrid single leg T-type converter are experimentally verified.**

Keywords—Single-leg T-type converter, double pulse testing, silicon carbide, hybrid, snubbers.

I. INTRODUCTION

To reduce carbon footprint, using more efficient electric technologies has been gaining much attention. The backbones of these electric technologies are power converters that connect between power source and grid. Hence, high power density converters (HPDCs) are adopted widely [1]. The pre-requisite for HPDC design is to increase the switching frequency for power conversion so that the sizes of magnetic components that form the bulk of the HPDC can be reduced. For applications with space constraints and harsh ambient temperature, power devices that can withstand high temperature is a primary requirement [2]. Hence, silicon carbide (SiC) has emerged as wide bandgap (WBG) power devices intended for both high power density and high temperature applications, such as electric vehicle (EV) and more electric aircraft (MEA) [3]. The ability of SiC devices to switch at high frequency paves the way for SiC power converters in HPDC designs [4-8] but they also cause potential electromagnetic interference (EMI) [9]. During the turn-off transition, the high di/dt leads to voltage overshoots due to the stray inductance. While in the half bridge circuit, the high dv/dt during the turn-on transition of one transistor affects the complimentary transistor via the Miller capacitance, which may lead to a momentary arm shoot through or crosstalk . Therefore, the fast switching speed of the SiC MOSFET increases the likelihood of EMI, as compared to conventional Si insulated-gate bipolar transistor (IGBT) [10, 11].

In the aircraft application of this paper, the T-type converter topology are selected to be an interface between DC bus and high-speed permanent magnet electric machines for high power density. Using a T-type converter with SiC and IGBT half-bridge modules as an example, the switching characteristics of the power modules will be studied based on double pulse testing (DPT), and the switching losses are also evaluated. The single leg T-type converter consists of a middle leg with two SiC half-bridge power modules or with one Si half-bridge power module, and a phase leg with one SiC half-bridge module [12, 13]. To improve the power density, three different power devices Cree CAS300M12BM2 SiC MOSFET, Semikron SKM350MB120SCH17 SiC MOSFET, and Semikron SKM300GM12T4 Si IGBT are proposed to be investigated and compared. In addition, due to the larger loop inductance of the middle leg, the switching ringing is required to be reduced for low electromagnetic interference (EMI) noise and easier control sampling. Snubbers such as resistor-capacitor RC snubber and resistor-capacitor-diode RCD snubber are common ways to suppress these ringing [14, 15]. The RC snubber is also proposed to suppress the switching ringing of middle leg in this single leg T-type converter. Finally, the function testing of the single leg T-type converter are operated.

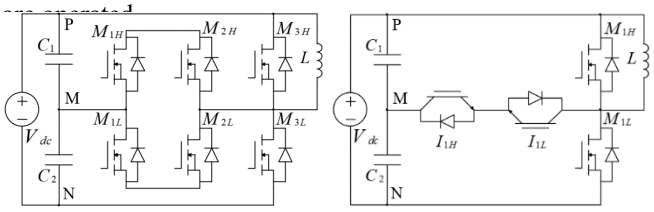

(a) (b)

Fig. 1. DPT circuit: (a) schematic for MOSFET of M_{2L} and diode of M_{3H}, or MOSFET of M_{3L} and diode of M_{3H}; (b) schematic for MOSFET of M_{1L} and diode of M_{1H}, or IGBT of I_{1L} and diode of M_{1H}.

II. T-TYPE CONFIGURATION FOR DOUBLE PULSE TESTING

Fig. 1 (a) presents the three SiC half bridge power modules single leg T-type converter, and Fig. 1 (b) shows the single leg T-type converter with one IGBT and one MOSFET half bridge power modules. DPT is a good way to evaluate the switching characteristics of a power module. The DPT is performed for the MOSFET of M2L and the diode of M3H, or the MOSFET of M3L and the diode of M3H with the configurations depicted in Fig. 1(a). Another DPT is performed for the MOSFET of M1L and the diode of M1H, or the IGBT of I1L and the diode of M1H with the configurations described in Fig. 1(b). The air-cored single layer inductor L is an air-cored inductor with low parasitic

978-1-5386-8136-7/18/$31.00

capacitance, and the switching characteristics of the other devices can be tested by the DPT with the air-cored single layer inductor connected in the low side of the phase leg devices.

III. CREE CAS300M12BM2 SIC MOSFET, SEMIKRON SKM350MB120SCH17 SIC MOSFET, AND SEMIKRON SKM300GM12T4 SI IGBT DEVICES

A. Comparison of Power Devices

Three different power devices for the single leg T-type converter are conducted and investigated: Cree CAS300M12BM2 SiC MOSFET, Semikron SKM350MB120SCH17 SiC MOSFET, and Semikron SKM300GM12T4 Si IGBT devices. All the devices have the packages for the gate driver and power terminals. Main devices parameters are listed in Table I. For HPDC, the most important factor is the lower losses of the devices, which means lower conduction losses with smaller on resistance, and lower switching losses with fast switching transition. Besides, the junction temperature and the thermal resistance are also two factors to limit the heatsink design. On the other hand, the smaller switching ringing is also required, which will reduce the size and weight of the EMI filter, and also decrease the switching losses. The ringing frequency $f_{ringing}$ mainly come from the parasitic capacitance C_{par} of devices, and the stray inductance L_{str} of devices, dc bus bar, and decoupling capacitors.

$$f_{ringing} = \frac{1}{2\pi\sqrt{C_{par} * L_{str}}} \quad (1)$$

TABLE I SIC MOSFET, AND SI IGBT DEVICES PARAMETERS

	Cree SiC MOSFET CAS300M12BM2	Semikron SiC MOSFET SKM350MB120SCH17	Semikron Si IGBT SKM300GM12T4
V_{ds}/V_{ce}	1200 V	1200 V	1200 V
I_d/I_c	404 A @25 ºC	523 A @25 ºC	422 A @25 ºC
$R_{DS\text{-}on}/R_{CE\text{-}on}$	5.0 mΩ @25 ºC	5.6 mΩ @25 ºC	3.5 mΩ @25 ºC
C_{iss}/C_{ies}	11.7 nF @600 V	34.48 nF @800 V	17.6 nF @25 V
C_{oss}/C_{oes}	2.55 nF @600 V	1.096 nF @800 V	1.16 nF @25 V
C_{rss}/C_{res}	0.07 nF @600 V	0.152 nF @800 V	0.94 nF @25 V
V_{GS}/V_{GE}	-5 V to +20 V	-6 V to +22 V	-20 V to +20 V
$V_{GS(th)}/V_{GE(th)}$	2.3 V	1.6 V to 4 V	5.8 V
Q_g	1025 nC @20 V	1512 nC @18 V	1700 nC @15 V
T_j	150 ºC	175 ºC	175 ºC
R_{jc}	0.075 ºC/W	0.045 ºC/W	0.11 ºC/W

B. Double Pulse Testing

The double pusle testing of the two kinds of single leg T-type converters in Fig. 2 are conducted, and Fig. 3 gives the experimental set up. The DC bus voltage is 540 V. The MOSFET is controlled by a digital signal processor TMS320F28335 with a double pulse signal. An air-cored single layer inductor is around 60 uH and used as the inductive load. The Tektronix THDP0200 200 MHz high voltage differential probe is utilized to measure the switching module voltage. The current transformer (CT) with 10 times ratio is applied to observe the load inductor current due to the limit range of lab current probe, and the CT will increase the additional switching loop inductance, which will induce a little bit difference between reality and measurement. The DPT voltage and current of the turn-on and turn-off transitions for the phase leg switches and the middle leg switches are measured in Fig. 4 and Fig. 5, respectively. It is easier to know that the ringing of the phase leg switches is much smaller than the ringing of the middle leg switches, due to the smaller switching loop stray inductance and the voltage dependent junction capacitances. Meanwhile, all the switching losses are tabulated in Table II and Table III. For the phase leg, the Cree SiC MOSFET CAS300M12BM2 almost has half of the switching losses, compared to Semikron SiC MOSFET SKM350MB120SCH17. For the middle leg, the switching losses of all the three devices have no much differences. To consider the power density, the Semikron Si IGBT SKM300GM12T4 for the middle leg is the best choice, which only needs one half bridge power modules, compared to two SiC power modules. Therefore, for the HPDC design, the single leg T-type converter with the hybrid of the Cree SiC MOSFET CAS300M12BM2 phase leg and the Semikron Si IGBT SKM300GM12T4 middle leg is the final selection.

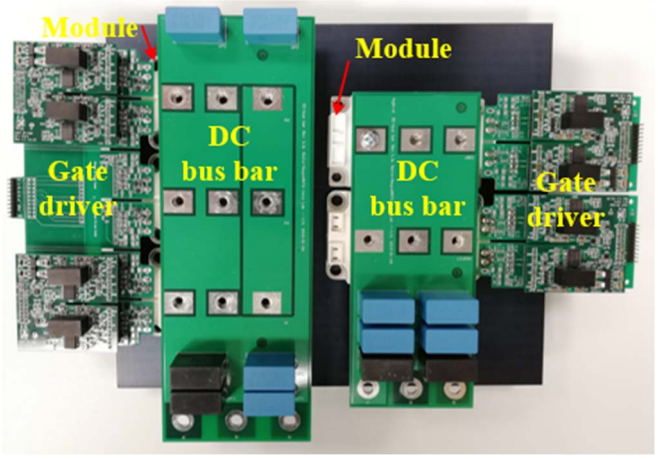

Fig. 2. Singel leg T-type converter prototypes: (a) All half bridge SiC MOSFET devices (left); (b) Hybrid devices of half bridge SiC MOSFET and Si IGBT (right).

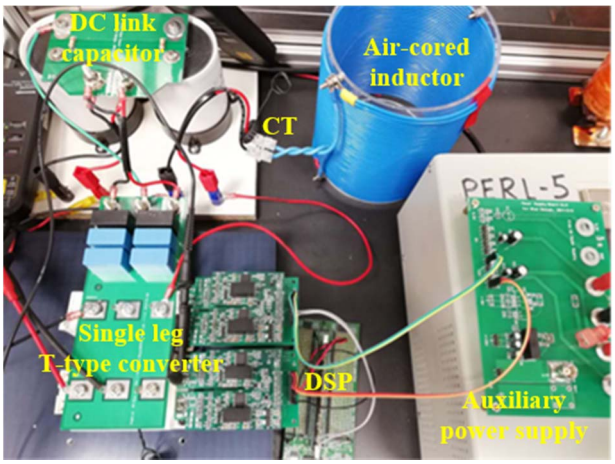

Fig. 3. Single leg T-type converter with half-bridge IGBT (SKM300GM12T4) and SiC (CAS300M12BM2) power modules

TABLE II OUTER LEG SWITCHING LOSSES (EXTERNAL GATE RESISTOR=5 Ω)

Type of devices	Eon	Eoff	Esw
CAS300M12BM2 (SiC)	15.953 mJ	10.281 mJ	26.234 mJ
SKM350MB120SCH17(SiC)	30.415 mJ	16.556 mJ	46.971 mJ

TABLE III MIDDLE LEG SWITCHING LOSSES (EXTERNAL GATE RESISTOR=5 Ω)

Type of devices	Eon	Eoff	Esw
CAS300M12BM2	9.642 mJ	3.499 mJ	13.141 mJ
SKM350MB120SCH17(SiC)	7.465 mJ	4.115 mJ	11.580 mJ
SKM300GM12T4 (IGBT)	8.006 mJ	5.698 mJ	13.704 mJ

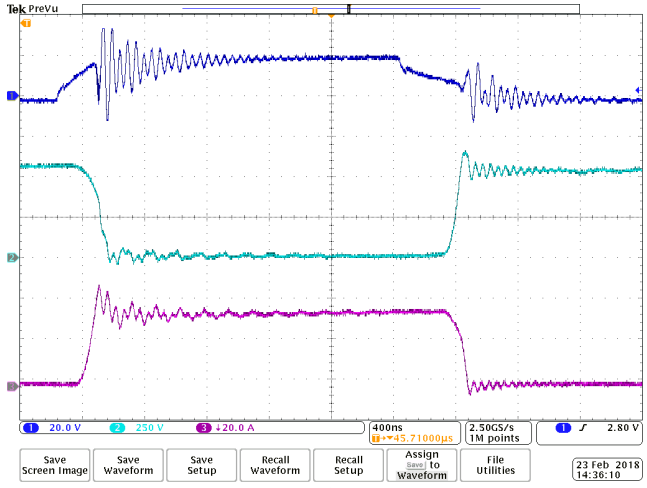

(a)

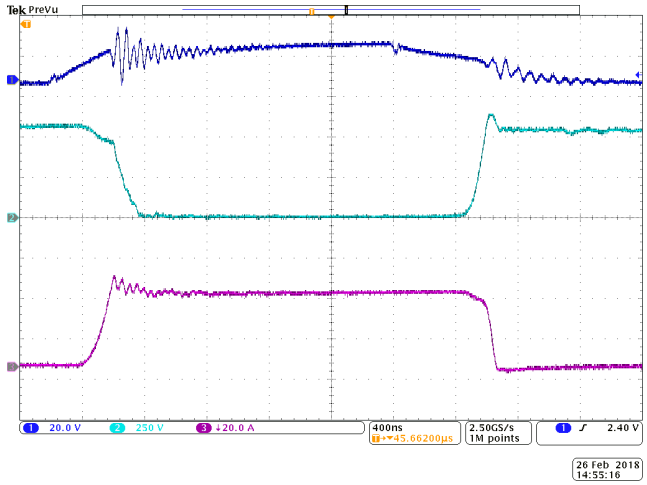

(b)

Fig. 4. Voltage and current waveforms of outer switches. (a) CAS300M12BM2. (b) SKM350MB120SCH17.

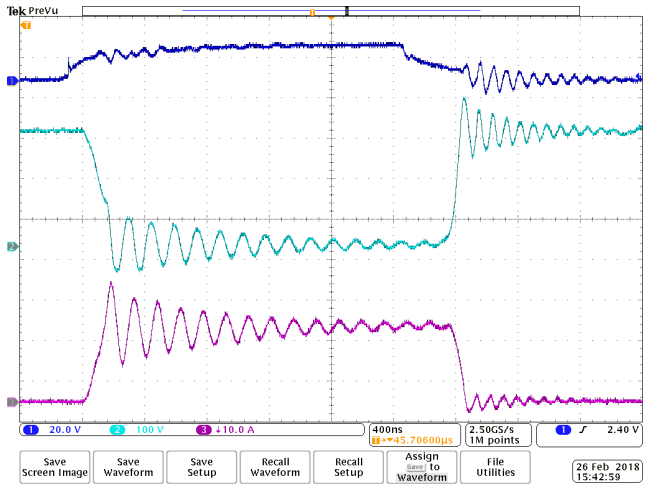

(a)

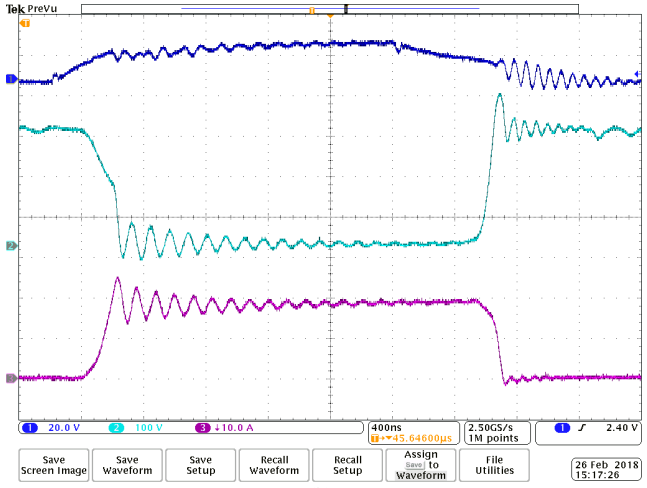

(b)

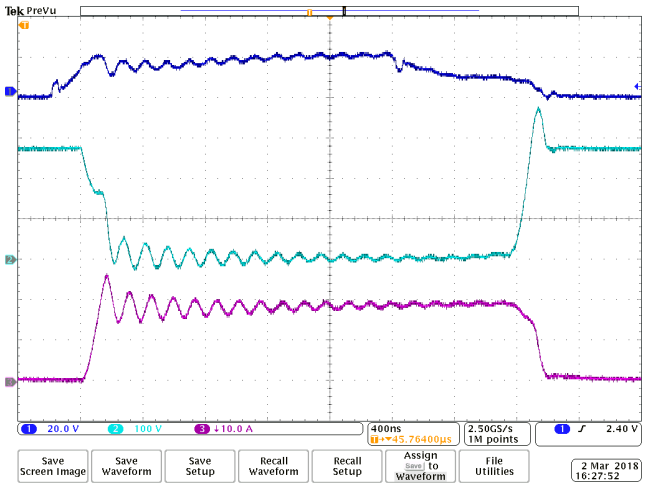

(c)

Fig. 5. Voltage and current waveforms of middle switches. (a) CAS300M12BM2. (b) SKM350MB120SCH17. (c) SKM300GM12T4.

IV. RC SNUBBER DESIGN

The RC snubber in this single leg T-type converter is to damp voltage and current ringing, which will reduce EMI noise, transfer power dissipation from the switch to the RC snubber, and facilitate the control sampling.

A. RC snubber calculation

RC snubber are an effective way of ringing suppression if appropriately designed. Fig. 6 presents the RC snubber connected in the middle leg of IGBT, and Fig. 7 shows the prototype of RC snubber, where the snubber resistors and capacitors are soldered on the PCB, and then terminals 1, 2, and 3 of the PCB are fixed on the power module directly. To achieve significant damping and with unknown of the parasitic capacitance C_{par} and the stray loop inductance L_{str}, a good quick choice is to make C_s equal to twice the sum of the output capacitance of the switch and the estimated mounting capacitance, and R_s is selected by [16],

$$Rs = \frac{V_{DS}}{I_o} \tag{2}$$

The power dissipated in R_s can be estimated from peak energy stored in C_s,

$$P_{R_s} = \frac{C_s V_{DS}^2}{2} \tag{3}$$

This is the amount of energy dissipated in R_s when C_s is charged and discharged so that the average power dissipation at a given switching frequency (f_s) is calculated by the formula (4). Therefore, in the real continuous operating of high power converter, the pawer rating of RC snubber needs to be considered again, compared to the RC snubber in Fig. 7..

$$W_{R_s} = \frac{C_s V_{DS}^2}{2} \cdot 2f_s = C_s V_{DS}^2 f_s \quad (4)$$

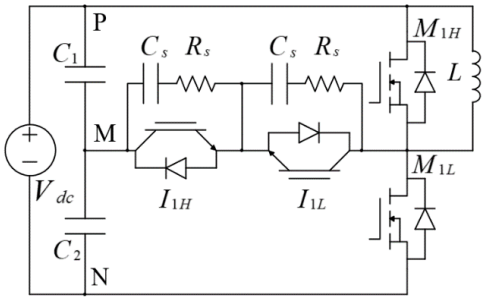

Fig. 6. DPT circuit with RC snubber.

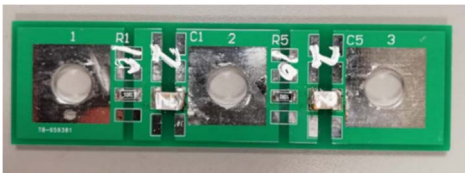

Fig. 7. RC snubber.

B. RC snubber verification

There are six combinations of RC snubbers as shown in Table IV, with two resistances and three capacitances. The 2 ohms resistor is selected by the formula (2), and the three capacitances are given to be adjusted, due to the unknown of the output capacitance at 270 V. The other 10 ohms resistor is used to verify the effectiveness of the 2 ohms resistor. Both voltage and current switching transitions in Fig. 8 are improved, compared to Fig. 5 (c). In addition, the switching losses are also measured in Table IV. When the RC snubber values are 2 ohms and 9.4 nF, the switching losses are the minimum among these combinations, and the waveforms of the voltage and current are also the smoothest.

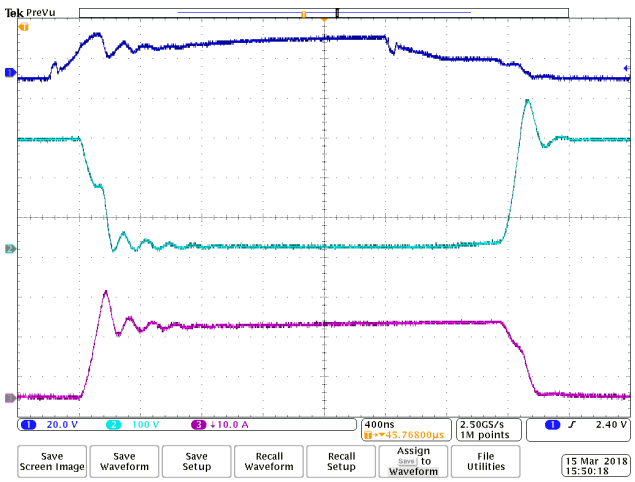

Fig. 8. Voltage and current waveforms of middle switches with RC (2 ohm, 9.4 nF) snubber in the hybrid sing leg T-type converter.

TABLE IV MIDDLE LEG SWITCHING LOSSES WITH RC SNUBBER IN FIGURE 6 (EXTERNAL GATE RESISTOR=5 Ω)

RC snubber	Eon	Eoff	Esw
RC (0 ohm, 0 nF)	7.826 mJ	5.425 mJ	13.251 mJ
RC (2 ohm, 2 nF)	8.040 mJ	5.638 mJ	13.678 mJ
RC (2 ohm, 4.7 nF)	6.124 mJ	5.413 mJ	11.537 mJ
RC (2 ohm, 9.4 nF)	4.817 mJ	5.417 mJ	10.234 mJ
RC (10 ohm, 2 nF)	6.581 mJ	5.191 mJ	11.772 mJ
RC (10 ohm, 4.7 nF)	5.672 mJ	5.208 mJ	10.880 mJ
RC (10 ohm, 9.4 nF)	6.180 mJ	4.982 mJ	11.162 mJ

V. FUNCTION TEST OF SINGLE LEG T-TYPE CONVERTER

The function testing of the selected hybrid single leg T-type converter are verified with the DC bus voltage of 200V, RL load of 143 uH and 200 ohms, and the switching frequency of 50 kHz. The results are presented in Fig. 9. It is clear that the single leg T-type converter works well, but a little bit unbalance of DC link capacitor voltage and the overshoot of output voltage will induce higher harmonics and electromagnetic interference. Therefore, neutral point voltage control and snubber for switching ringing suppression are required to obtain high quality output voltage in the practical application.

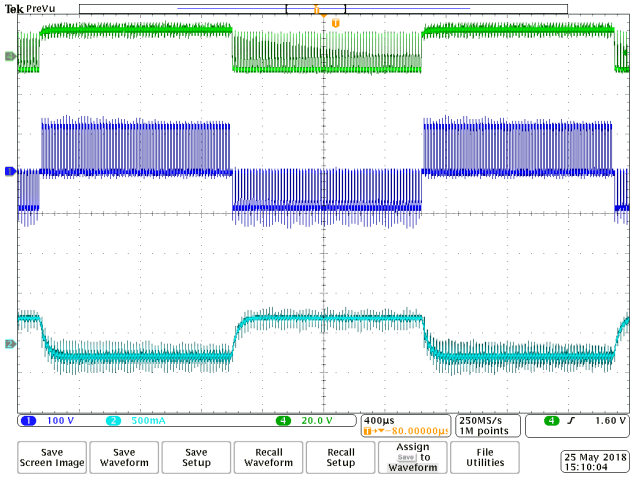

Fig. 9. Gate driver voltage (Channel 4), output voltage (Channel 1), and output current (Channel 2) waveforms of sing leg T-type converter.

VI. CONCLUSIONS

In this paper, to improve the power density, a one hybrid single leg T-type converter with one SiC half bridge power modules and one IGBT half bridge power module are proposed and investigated. Firstly, the double pulse testing is used to verify the advantage of the hybrid single leg T-type converter with around two-thirds weight and size, compared to the full SiC single leg T-type converter. Secondly, to suppress the switching ringing of the middle leg switch, the RC snubber is proposed and investigated with different experimental verifications. Finally, the function testing of the selected hybrid single leg T-type converter are carried out.

ACKNOWLEDGMENTS

This research work was conducted in the Rolls-Royce@NTU Corporate Lab with funding support from the National Research Foundation (NRF), Rolls-Royce and Nanyang Technological University; under the Corp Lab@University Scheme.

REFERENCES

[1] A. Nawawi, C. F. Tong, S. Yin, A. Sakanova, Y. Liu, Y. Liu*, et al.*, "Design and Demonstration of High Power Density Inverter for Aircraft Applications," *IEEE Transactions on Industry Applications,* vol. 53, pp. 1168-1176, 2017.

[2] B. S. Bhangu and K. Rajashekara, "Electric starter generators: Their integration into gas turbine engines," *IEEE Industry Applications Magazine,* vol. 20, pp. 14-22, 2014.

[3] Z. Chen, Y. Yao, D. Boroyevich, K. D. Ngo, P. Mattavelli, and K. Rajashekara, "A 1200-V, 60-A SiC MOSFET multichip phase-leg module for high-temperature, high-frequency applications," *IEEE Transactions on Power Electronics,* vol. 29, pp. 2307-2320, 2014.

[4] C. Tong, A. Nawawi, Y. Liu, S. Yin, K. Tseng, Y. Liu*, et al.*, "Challenges in switching waveforms measurement for a high-speed switching module," presented at the Conf. of 2015 IEEE Energy Conversion Congress and Exposition (ECCE), Montreal, Canada, September 20-24, 2015.

[5] S. Yin, K. J. Tseng, R. Simanjorang, Y. Liu, and J. Pou, "A 50-kW high-frequency and high-efficiency SiC voltage source inverter for more electric aircraft," *IEEE Transactions on Industrial Electronics,* vol. 64, pp. 9124-9134, 2017.

[6] Y. Liu, K.-Y. See, S. Yin, R. Simanjorang, C. F. Tong, A. Nawawi*, et al.*, "LCL Filter Design of a 50-kW 60-kHz SiC Inverter with Size and Thermal Considerations for Aerospace Applications," *IEEE transactions on Industrial Electronics,* vol. 64, pp. 8321-8333, 2017.

[7] Y. Liu, K. Y. See, K. J. Tseng, R. Simanjorang, and J.-S. Lai, "Magnetic integration of three-phase LCL filter with delta-yoke composite core," *IEEE transactions on Power Electronics,* vol. 32, pp. 3835-3843, 2017.

[8] Y. Liu, K. Y. See, R. Simanjorang, Z. Y. Lim, and Z. Y. Zhao, "Modeling and simulation of switching characteristics of half-bridge SiC power module in single leg T-type converter for EMI prediction," presented at the Conf. of 2018 IEEE International Symposium on Electromagnetic Compatibility and 2018 IEEE Asia-Pacific Symposium on Electromagnetic Compatibility (EMC/APEMC), Singapore, June 20-23, 2018.

[9] X. Gong and J. A. Ferreira, "Investigation of conducted EMI in SiC JFET inverters using separated heat sinks," *IEEE transactions on Industrial Electronics,* vol. 61, pp. 115-125, 2014.

[10] Y. Shi, R. Xie, L. Wang, Y. Shi, and H. Li, "Switching characterization and short-circuit protection of 1200 V SiC MOSFET T-type module in PV inverter application," *IEEE Transactions on Industrial Electronics,* vol. 64, pp. 9135-9143, 2017.

[11] E. Gurpinar and A. Castellazzi, "Single-phase T-type inverter performance benchmark using Si IGBTs, SiC MOSFETs, and GaN HEMTs," *IEEE Transactions on Power Electronics,* vol. 31, pp. 7148-7160, 2016.

[12] A. Deshpande and F. Luo, "Multilayer busbar design for a Si IGBT and SiC MOSFET hybrid switch based 100 kW three-level T-type PEBB," presented at the Conf. of 2017 IEEE 5th Workshop on Wide Bandgap Power Devices and Applications (WiPDA), Albuquerque, NM, Octber 30- Novmeber 1, 2017.

[13] J. He, R. Katebi, N. Weise, N. A. Demerdash, and L. Wei, "A Fault-Tolerant T-Type Multilevel Inverter Topology With Increased Overload Capability and Soft-Switching Characteristics," *IEEE Transactions on Industry Applications,* vol. 53, pp. 2826-2839, 2017.

[14] K. Yatsugi, K. Nomura, and Y. Hattori, "Analytical Technique for Designing an RC Snubber Circuit for Ringing Suppression in a Phase-Leg Configuration," *IEEE Transactions on Power Electronics,* vol. 33, pp. 4736-4745, 2018.

[15] Y. Yamashita, J. Furuta, S. Inamori, and K. Kobayashi, "Design of RCD snubber considering wiring inductance for MHz-switching of SiC-MOSFET," presented at the Conf. of 2017 IEEE 18th Workshop on Control and Modeling for Power Electronics (COMPEL), Padova, Italy, July 9-12, 2017.

[16] R. Severns and E. Reduce, "Design of snubbers for power circuits,". [online]. Available: http://www.cde.com/resources/technical-papers/design.pdf